www.czasopisma.pan.pl PAN POLSKA AKADEMIA NAUK www.journals.pan.pl

A R C H I V E S O F M E T A L L U R G Y A N D M A T E R I A L S

Volume 57 2012 Issue 4

DOI: 10.2478/v10172-012-0129-x

H. PAUL*, L. LITYŃSKA-DOBRZYŃSKA*, M. MISZCZYK*, M. PRAŻMOWSKI**

MICROSTRUCTURE AND PHASE TRANSFORMATIONS NEAR THE BONDING ZONE OF Al/Cu CLAD MANUFACTURED BY EXPLOSIVE WELDING

ZMIANY MIKROSTRUKTURALNE I FAZOWE W POBLIŻU STREFY POŁĄCZENIA UKŁADU WARSTWOWEGO Al/Cu WYTWORZONEGO TECHNOLOGIĄ ZGRZEWANIA WYBUCHOWEGO

The structure near the interface of bimetallic strips strongly influences their properties. In this work, the interfacial layers of explosively welded aluminium and copper plates were investigated by means of a scanning electron microscope (SEM), equipped with a high resolution system for local orientation measurements (SEMFEG/EBSD), and a transmission electron microscope (TEM), equipped with energy dispersive spectrometry (EDX) for the analysis of chemical composition changes.

The SEMFEG/EBSD-based local orientation measurements in the areas close to the interface, in both sheets, revealed fine-grained layers characterized by the clearly marked tendency of the copper-type rolling texture formation. The texture was described by an increased density of the orientations near the {112}<111>, {123}<634>and {110}<112>positions. The internal microstructure of the intermetallic inclusion is mostly composed of dendrites. The electron diffractions and the TEM/EDX chemical composition measurements in the intermetallic inclusions revealed only crystalline phases, both equilibrium and 'metastable'. Additionally, no significant regularity in the phase distribution with respect to the parent sheets was observed.

Keywords: intermetallic inclusion, interface, transmission electron microscopy, orientation mapping, explosive welding

Mikrostruktura w pobliżu strefy połączenia silnie wpływa na własności układów bimetalowych. W niniejszej pracy analizie poddano układy warstwowe Al/Cu wytworzone technologią zgrzewania wybuchowego. Badania prowadzono z wykorzystaniem skaningowej mikroskopii elektronowej wyposażonej w wysokorozdzielczy system pomiaru orientacji lokalnych oraz transmisyjnej mikroskopii elektronowej wyposażonej w analizator składu chemicznego. Systematyczne pomiary orientacji lokalnych w pobliżu strefy połączenia, w obydwu łączonych płytach, ujawniają formowanie się strefy silnie rozdrobnionych ziaren. Strefa ta scharakteryzowana jest przez formowanie się tekstury walcowania typu miedzi z dobrze uwidocznionymi składowymi zbliżonymi do położeń: {112}<111>, {123}<634> oraz {110}<112>. Wewnętrzna struktura 'intermetalicznych inkluzji' zbudowana jest z dendrytów. Badania z wykorzystaniem elektronowej mikroskopii transmisyjnej dokumentują, że wewnątrz strefy przetopień następuje formowanie się faz krystalicznych, zarówno równowagowych jak i 'metastabilnych'. Skład chemiczny formujących się faz nie wykazywał związku z położeniem ziaren względem płyt bazowych.

1. Introduction

Explosive welding is a solid state metal joining process used to create a metallurgical bond between two similar or dissimilar metals [1]. A weld joint is produced by means of a high velocity impact of one metallic mass onto another, aided by a controlled detonation with an explosive charge. In explosive welded plates at the collision point, the perfectly clean surfaces are brought together under very high pressure. The high velocity oblique collision will 'produce' high temperature and high shear strain near the collision point in a very short time. This causes local melting of the bonded metals, simultaneously with the local plastic deformation. The very short time of the heat influence, due to the high thermal conductivity of the metals, leads to high cooling rates and thus, in the solidification process, the melted metals are 'transformed' to brittle intermetallic of different compounds, e.g. [2-11].

Explosive weld microstructures have been examined for half a century. In these works, the techniques of optical microscopy, scanning electron microscopy (SEM) and mechanical testing were used for the microstructural analyses and the clad properties' characterization. Particular attention was paid to the description of the influence of the technological parameters, such as the

* INSTITUTE OF METALLURGY AND MATERIALS SCIENCE PAS, KRAKÓW, 25 REYMONTA ST., POLAND

** OPOLE UNIVERSITY OF TECHNOLOGY, FACULTY OF MECHANICS, OPOLE, 5 MIKOŁAJCZYKA ST., POLAND

detonation energy, the distance between the plates and the inclination angle of the flyer plate, on the '*quality of the weld*', e.g. [1, 2-6]. Despite the fact that the literature data, based on SEM analyses, is relatively rich, there are only few works dealing with the textural transformations occurring in the parent sheets close to the interface, e.g. [11, 12].

A strongly limited number of publications has been issued also on the nano- scale transmission electron microscopy (TEM) analyses of the phenomena that occur within the intermetallic inclusions. They were limited to selected metal compositions, e.g. the steel/Ti clad [2, 10], Ti/Ti clad [13], copper to copper clad [2] or a Ni-based amorphous or metallic glass film clad on stainless steel [14]. However, among those works,only the paper by Song et al. [10] on the steel to Ti clad soundly characterizes the nano-scale events observed inside the intermetallic inclusion. Nothing has been done, to our knowledge, in respect to a detailed microstructure characterization of the intermetallic inclusions of the Cu/Al clad and the parent materials close to the interface. It is, therefore, the aim of this work to characterize, at the micro-/nano- scale, the events that occur near the interface in the Cu/Al cladding system.

This work analyses two aspects of the changes that occur near the interface of explosively welded sheets. On the one hand, the texture and microstructure changes that occur close to the interface in explosively welded aluminium and copper sheets were analysed by means of a SEM equipped with a high resolution electron backscattered (EBSD) facility. On the other hand, the investigations of the reaction products formed at the cladding interface were carried out by means of TEM. The quite different electrochemical properties of the bonded metals necessitated the application of the focus ion beam (FIB) technique for the thin foil preparation from the areas covering the interfaces. Finally, the events occurring during the intermetallic phase's formation under dynamic loading (explosive bonding) were discussed in relation to those observed in the static terms of ageing, after the application of other bonding techniques.

2. Materials and experimental procedures

2.1. Materials and initial microstructure of sheets

The explosion welded materials evaluated in this study were a standard explosion clad product produced by High Energy Technologies Works 'Explomet' (Opole, Poland). Commercial purity aluminium (AA1050) and copper (M1E-99.5%) were used to manufacture the Al/Cu composites for electrotechnical applications. The thickness of the base (Al) and the flyer (Cu) plates were 25 mm and 3 mm, respectively, whereas their width and length were 2000 mm×4000 mm. The surfaces of the plates were used as-received. The composites were obtained by means of the constant stand-off explosive cladding technique. A detonator was placed in the middle of the plate's width close to one of the edges. In the middle of the plate's width, the jetting direction was parallel to the rolling direction (RD). The stand-off distance was 3 mm, whereas the measured explosive detonation velocity was 2200 m/s. Samples for further microscopic observations were cut-off from the end parts of the sheet.

2.2. Meso- scale analyses based on SEM/EBSD

The microstructures of the parent sheets (before and after cladding) were analyzed in the section perpendicular to the transverse direction (TD) with the use of a JEOL 6500F scanning electron microscope, equipped with a field emission gun and an electron backscattered diffraction facility. The microscope control, the pattern acquisition and the indexing were performed with the use of the HKL Channel 5 software. The orientation maps were created in the beam-scanning mode with the step size ranged between 50 nm and 500 nm. Before cladding, the copper plates (in the ND-RD section, where: ND is the normal direction), were characterized by the equiaxed grains, with the average grain diameter of 30 μm. The aluminium plate (in the same section) was characterized by a microstructure typically observed after hot rolling, i.e. composed of layers of very flat grains. The (average) dimensions of the elongated grains along the longer and the shorter axes equalled about 100μm and 15μm, respectively (Fig. 2).

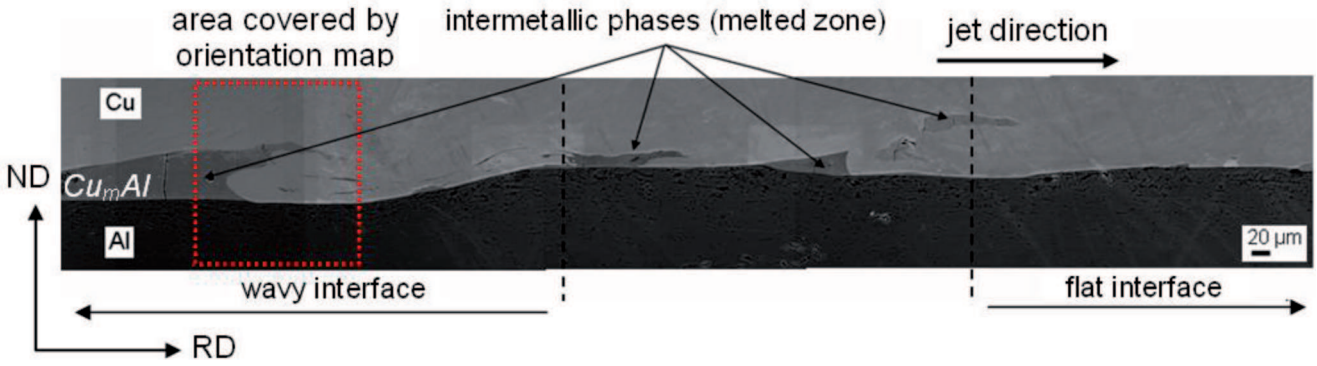

Fig. 1. The 'wavy character' of the interface and the formation of melting zones at the crest of the waves. SEM image in the Back Scattered Electron mode. ND-RD section [16]

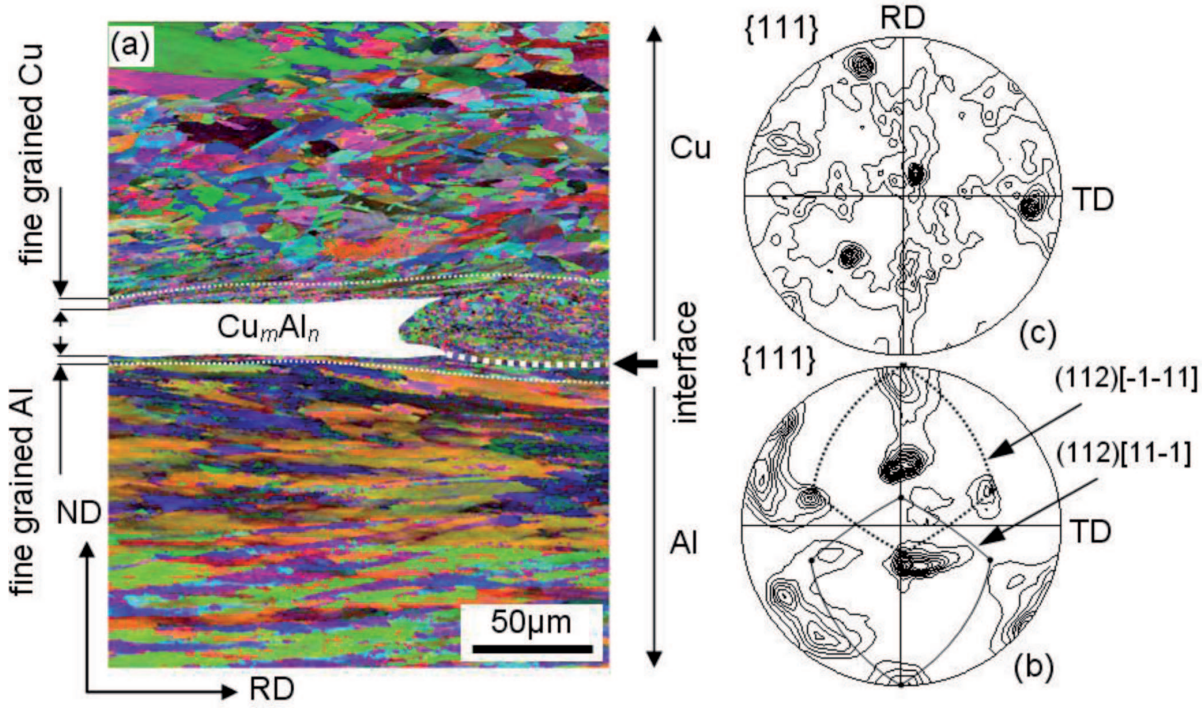

Fig. 2. (a) SEMFEG/EBSD orientation map showing the microstructure close to the interface. The map corresponds to SEM-BSE micrographs presented in Fig. 1 (marked area). The {111} pole figures calculated for (b) Aland (c) Cu layers. ND-RD section. SEMFEG/EBSD local orientation measurements. Step size of 200 nm

2.3. TEM analysis of structure and chemical composition changes in the intermetallic inclusion

The microstructure observations and the chemical composition measurements were performed by means of TEM with the use of a FEI Technai G^2 microscope, operating at the accelerating voltage of 200kV. The TEM was equipped with a field emission gun and a high-angle annular dark field scanning/transmission detector (HAADF/STEM), combined with an EDAX^{TM} energy dispersive X-ray (EDX) microanalyser. The resolution of the TEM/EDX system was ~1nm. Due to the quite different electrochemical properties of the welded metals, the classic technique of thin foil preparation by means of electrolytic polishing was not adequate here. Therefore, for the nano- scale analyses of the microstructural and the chemical composition changes across the interface, the FIB cutting was applied for the thin foils preparation along the ND-TD section. In that case, the FEI FIB (FB2000A) instrument operating at 30kV was used.

3. Results

The cases of '*well-welded*' sheets were analyzed in this work. A macroscopically acceptable weld was produced, since the strength of the weld was higher than the

strength of the weaker one of the two components. Additionally, the electrical conductivity was at an acceptable level. In the case of the Cu/Al clad, the electrical conductivity is, beside the strength, one of the most important properties in industrial applications. The conductivity of intermetallic compounds is about one-seventh of the conductivity of copper and one-fifth of the conductivity of aluminium and depends on the exact chemical composition of the intermetallic phase [15]. This indicates that the total conductivity sharply decreases, due to the intense formation of volumes of solidified liquid.

In the present case, the applied technological settings of bonding 'produced' interfaces with only a small number of intermetallic inclusions. However, for practical reasons, the areas covering the relatively thick intermetallic inclusions were found and selected for further TEM-based analyses, as presented in Fig. 1a.

3.1. Macro- scale morphology of the interfacial zone

The morphology of the present joint was characterized by the mixture of wavy and flat patterns. A significant part of the interface was without intermetallic inclusions. The latter, if they occurred, were preferentially located near the front slope of the waves or within the vortex of the waves. The presence or absence of the intermetallic inclusions led to the 'creation' of one of the two types of interface, i.e. pure metal-solidified melt or pure metal-pure metal. The interfaces around the intermetallic inclusions were always very sharp. This suggests strong chemical composition changes across the boundary.

3.2. Microstructure and texture changes close to and far from the interface

The microstructure and texture across the interface were characterized by means of the local orientation measurement system. Two characteristic places within the samples in the 'after bonding' state, i.e. the areas located across the interface (including the areas covering the crest of the wave) and the areas distanced 1.5mm from the interface, were analyzed in detail.

Figure 2a shows the orientation map presented as a 'function' of the IPF colour code made across the interface. The map (from area marked in Fig. 1) clearly reveals the differences observed in the microstructure of both welded metals. The structure of the Al sheet near the interface is composed of deformed large grains[1)] elongated along RD, within the analysed area. The grains were deformed nearly to the same extent, except for the very thin layers directly adhering to the interface. The {111} pole figure corresponding to this part of the orientation map contains the maxima (of different intensity) located close to the main copper-type texture components, i.e. {112}<111>and {123}<634>with the scattering towards the {110}<112>and {110}<111>orientations[2)] (Fig. 2b). The copper sheet shows more or less elongated grains, but not to the same extent as those observed in the case of aluminium. However, this directionality in the grain geometry (in both metals) was very quickly lost as the distance from the interface increased. Finally, in the areas distanced about 200-250μm from the interface, nearly globular grains were observed, but still with the increased density of the dislocations inside the grains' interior. Near the interface, similarly to the case of aluminium, a strongly refined structure is observed. The texture corresponding to the area of the copper sheet was weak, as presented in Fig. 2c. Only one stronger texture component was observed close to {111}<112>orientation, probably due to the preference in the orientation distribution of the initial grains.

The formation of the extremely fine-grained structure near the interface is the common characteristic feature observed in both sheets. In the Al sheet, the thickness of the fine-grained layer was ~5μm, whereas in the case of Cu, this layer was significantly broader and its width ranged between 30μm and 80μm. Additionally, the orientation maps clearly show that the grains were separated by large angle grain boundaries with the misorientations higher than 15°. Although the total thickness of this fine-grained zone did not exceed a few or few tens of microns, these layers showed the well-marked copper-type texture, typically observed in highly deformed fcc metals. The orientations identified inside the fine-grained layers are presented in Figs. 3a and b. It is well-visible that the {111} pole figures contain the 'elements' of the standard copper-type rolling texture, dominated by two nearly complementary components close to the {110}<112> orientation (Figs. 3a and b).

The strongly refined structure is especially well-observed inside the areas of the waves that occurred in the copper sheet, as presented in Figure 4a. This map, made with the step size of 50nm, is presented as a 'function' of the quality of diffraction pattern. It

[1)] It is important to note that the average grain sizes of the initial materials were 200μm and 50μm for the aluminium and the copper sheets, respectively

[2)] The indices {*hkl*}<*uvw*>represent the texture component which has the {*hkl*} plane parallel to the RD-TD plane and the <*uvw*> direction parallel to RD

is well visible that the crest of the waves was composed of very thin (with the thickness below 200nm) and elongated grains, separated by large angle grain boundaries with the misorientations higher than 15°. These thin grains were strongly curved inside the crest of the wave and imitated well the rotational character of the material (copper) displacement during the wave formation, i.e. reflecting the non-homogeneous flow in the copper sheet close to the interface. Although the total thickness of this fine-grained zone did not exceed a few microns, the layers showed well-marked copper-type texture components. This effect is typically observed in the highly deformed face centred cubic metals.

The misorientation distribution close to the interface changes greatly between both plates, due to the progressive built up in the misorientations above 15° in the Cu plate (Fig. 5a). In the Al plate, the large fraction of the low-angle boundaries with the misorientation angles near the 10-15° is still dominant (Fig. 5b).

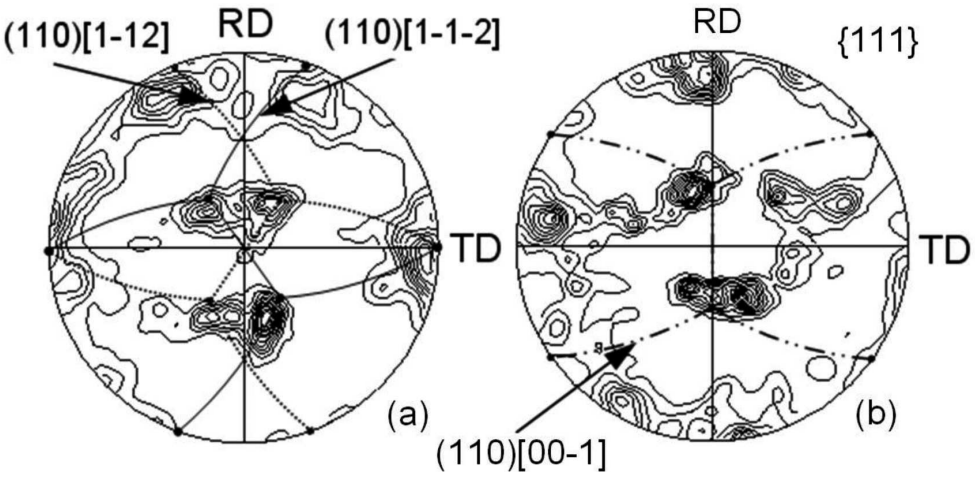

Fig. 3. The {111} pole figures calculated forfine-grained layersnear the interface – (a) Al and (b) Cu, corresponding to the orientation map presented in Fig. 2a. ND-RD section. Step size of 200nm. SEMFEG/EBSD local orientation measurements

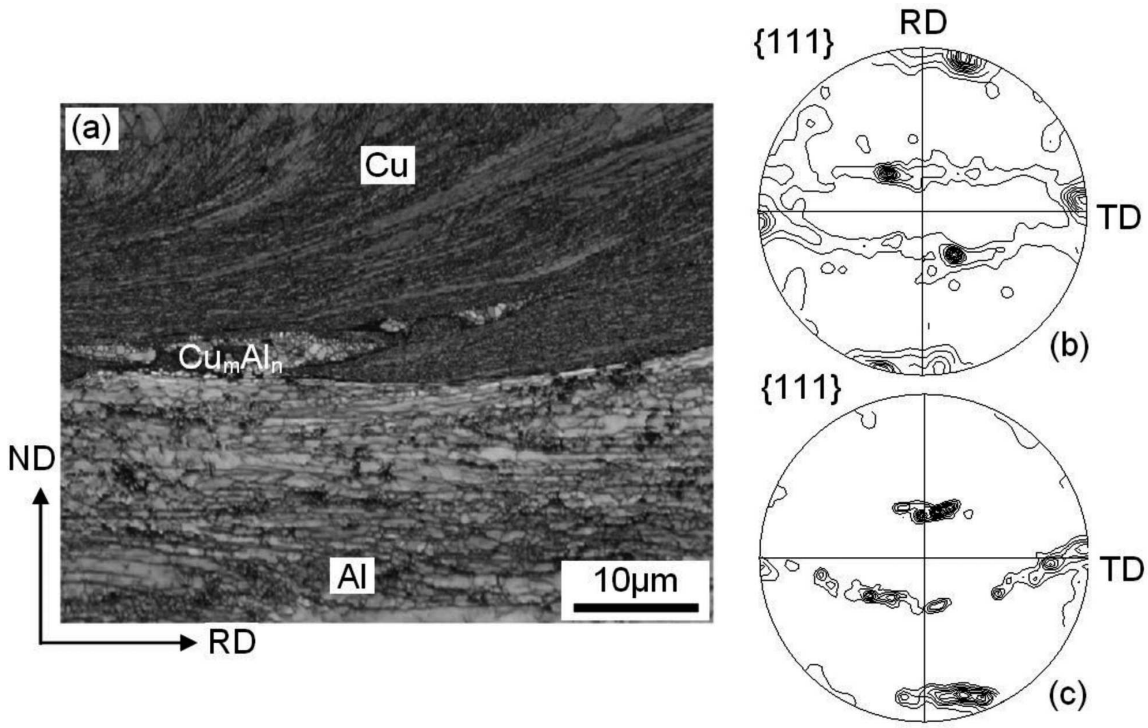

Fig. 4. (a) Orientation map displayed as a 'function' of the diffraction patterns quality (white areas – good quality, dark – poor quality) and corresponding {111} pole figures for Cu (b) and Al (c) sheets. ND-RD section. SEMFEG/EBSD local orientation measurements. Step size of 50nm

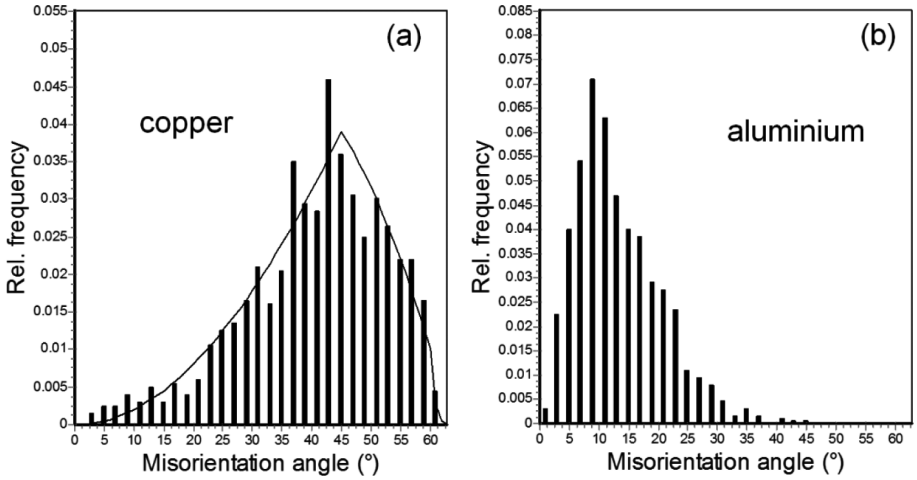

Fig. 5. Relative frequency of the grain boundaries' occurrence within particular class of misorientation angles, calculated separately for both sheets. (a) Nearly random distribution of grain boundaries (with large fraction of high-angle boundaries) in copper. (b) Increased fraction of low-angle grain boundaries in aluminium. The graphs correspond to the orientation map presented in Fig. 4

The 'intensity' of the plastic deformation decreases as the distance from the interface increases. In the copper plate, in the areas distanced ~1.5mm from the interface, the grains are nearly equiaxed and their interior is characterized by only a slightly increased density of the dislocations. This is visible as an increased density of the low angle boundaries (Fig. 6a and c). In the aluminium plate, for the same distance from the interface, the subdivision of the large grains is still visible (Fig. 6b and d). Figures 6a and b show the misorientation maps, where the whiter area marks the higher misorientation and thus the higher stored energy. They clearly show that, for the copper plate, the higher misorientations are connected with the areas placed near the grain boundaries and the grain interiors, whereas in aluminium - only with the (sub)grains boundaries. In the case of the copper plate, the texture is weak (Fig. 7a), whereas in the case of aluminium, only one stronger component near the {116}<331>orientation is observed (Fig. 7b), probably due to the orientation of the initial large grain.

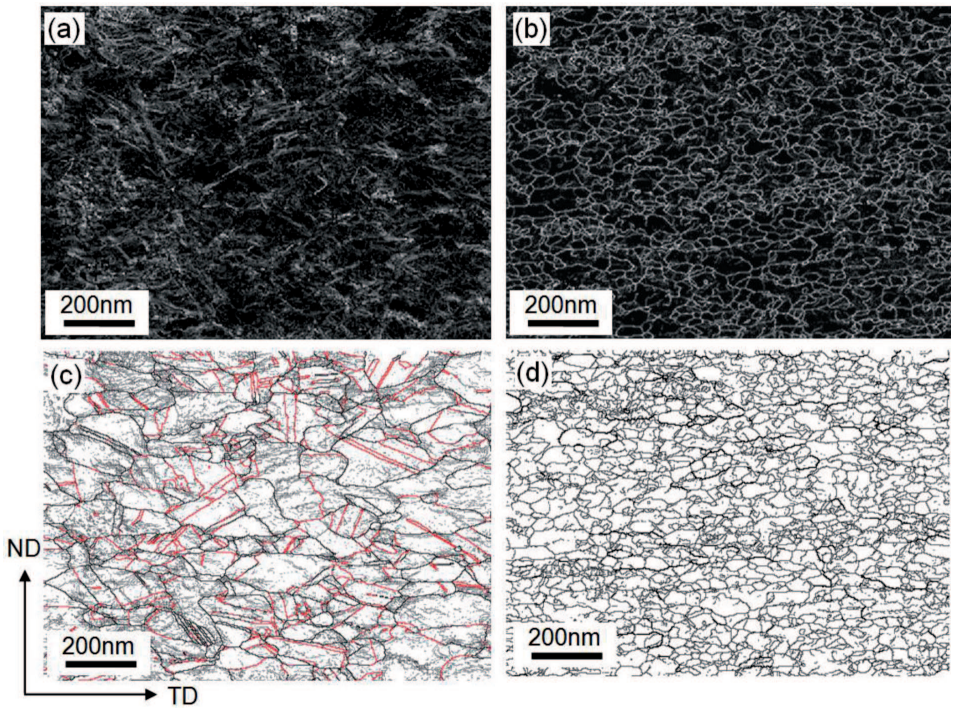

Fig. 6. Microstructure of the parent sheets in areas distanced 1.5mm from the interface. (a) and (b) distribution of misorientations (the brighter area the greater misorientation), (c) and (d) distribution of grain boundaries (thin and thick black lines represents low (<15°) and high (>15°) angle grain boundaries, respectively, whereas red lines – twin boundaries). (a) and (c) copper sheet, (b) and (d) aluminium sheet. ND-RD section. SEMFEG/EBSD local orientation measurements. Step size of 200nm

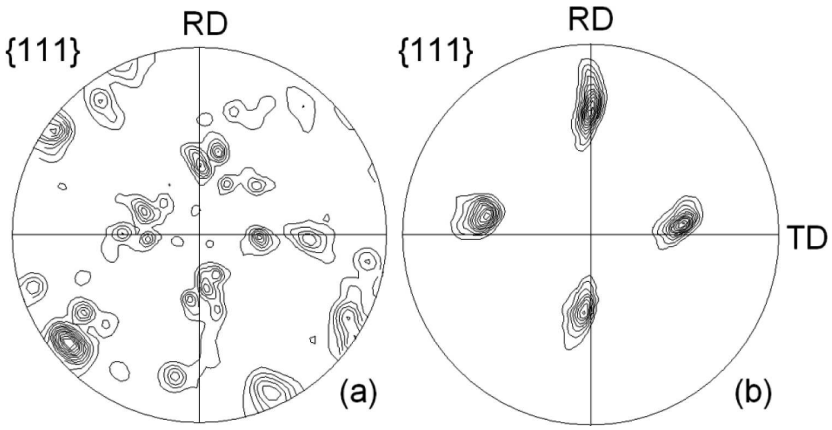

Fig. 7. Texture of the parent sheets in the areas distanced 1.5 mm from the interface. The {111} pole figures corresponding orientation maps presented in Fig. 6. (a) Cu and (b) Al sheet. ND-RD section. SEMFEG/EBSD local orientation measurements. Step size of 200nm

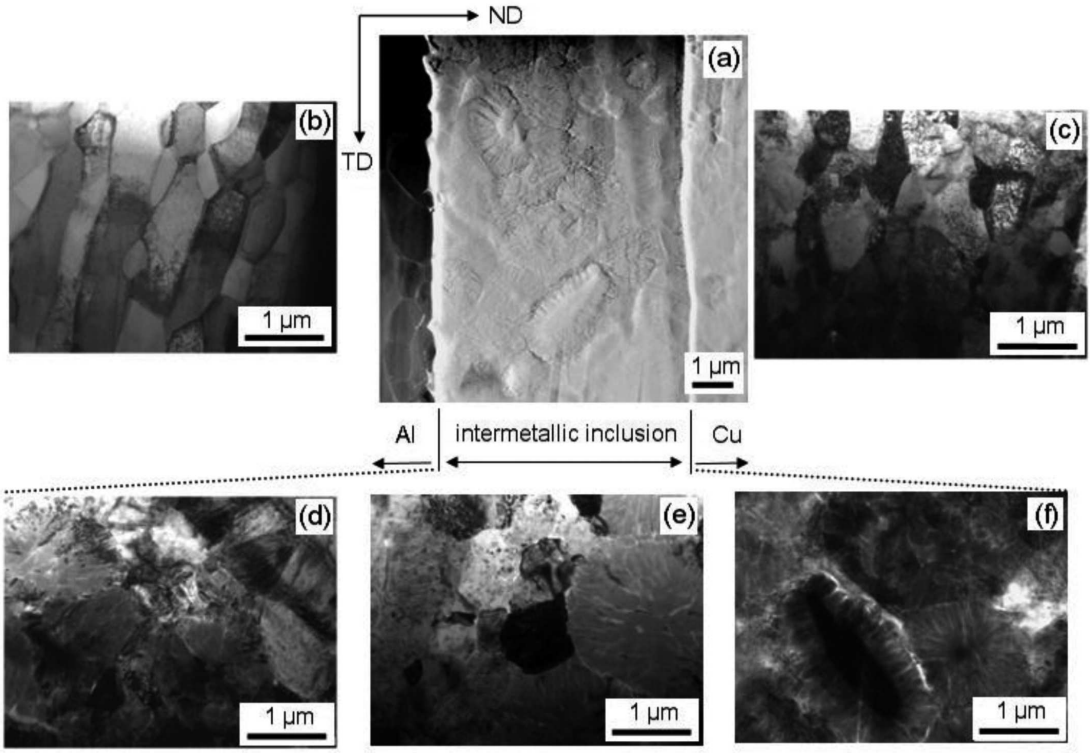

Fig. 8. Microstructural changes across the interfacial zone. (a) HAADF-STEM microstructure showing interfacial zone with intermetallic inclusion. The parent sheets microstructures in areas directly adhering to the intermetallic inclusion: (b) aluminium and (c) copper. (d) – (f) TEM bright field images showing dendrites inside the intermetallic inclusion. TEM imaging in ND-TD section

3.3. Microstructure of the interfacial zone

A detailed TEM microstructure characterization of the interfacial zones was performed on thin foils prepared by means of the FIB technique. Figure 8a shows the typical HAADF-STEM micrographs across the whole thickness of the intermetallic layer and the areas of the parent sheets directly adhering to the interfaces. In the present case, the thin foil was cut off the sample area containing a ~6μm thick intermetallic zone. As expected, two distinct interfaces of the pure metal-intermetallic inclusion type, clearly separating the Al and Cu sheets, were observed. It is visible that the microstructures of the Al and Cu sheets were different in the areas directly adhering to the intermetallic layer.

In aluminium, regular dislocation arrangements forming the (sub)grain structure are visible (Fig. 8b). The (sub)grains'[3)] length was of the order of a few microns,

[3)] It should be noted that the bright field imaging counts all types of boundaries, i.e. low- and high- angle, without distinction

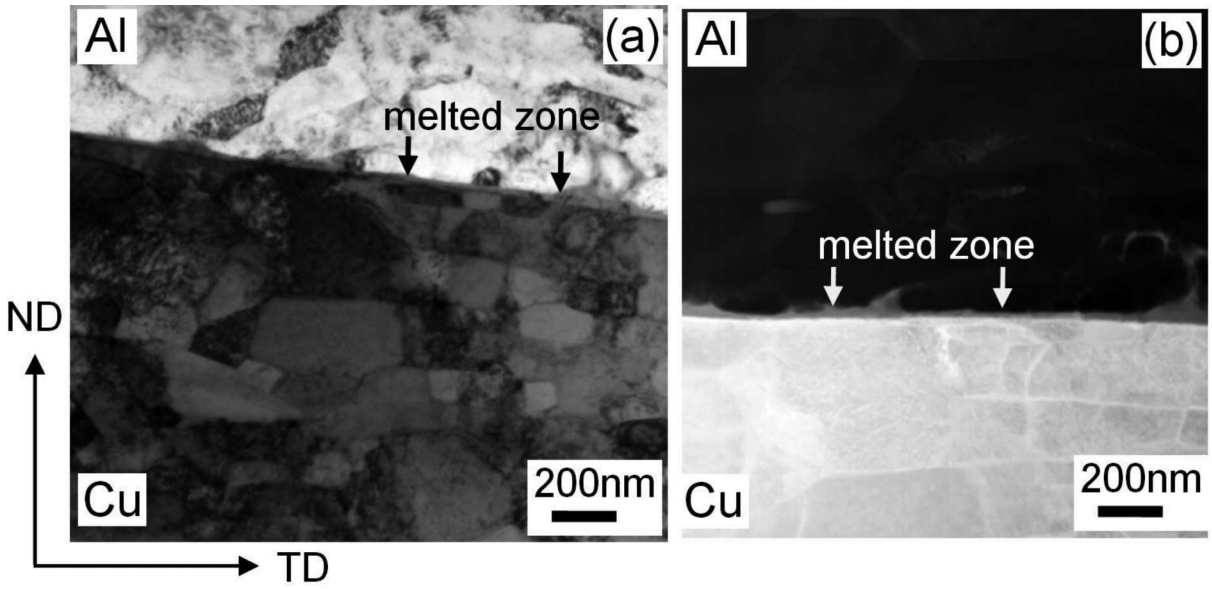

Fig. 9. Microstructural changes across the interface in the areas without macroscopically visible intermetallic inclusion. (a) Bright field micrographs showing interfacial zone with very thin layer of the solidified melt (melted zone) and corresponding (b) HAADF-STEM microstructure. TEM imaging in ND-TD section

whereas their width ranged between 200nm and 400nm. In the Cu sheet, the microstructure was composed of small, nearly equiaxed grains, with recrystallization twins and randomly distributed dislocations. The diameter of these grains ranged between 0.5μm and 1μm. The elongated shape of the (sub)grains in the Al sheet and the randomly distributed dislocations in the Cu sheet clearly indicated that during the welding, the deformation processes were prevailing over the softening ones.

The internal structure of the intermetallic inclusion is quite different with respect to the microstructures observed in the parent sheets. Some of the grains resemble dendrites with a clearly marked core and arms, as visible in Fig. 8a and Figs. 8d-f. The diameter of these grains ranged between 0.5μm and 2μm. They showed a typical crystalline contrast during the tilting in TEM.

In the case of the pure metal-pure metal interface (Fig. 9), the structure of the parent sheets near the interface was finer than that observed near the intermetallic inclusion-pure metal interface. Additionally, the interior of the cells or the grains was intensely filled with randomly distributed dislocations. At higher magnifications, the very thin layer of the solidified melt which covered almost the whole interface, was well-visible. The TEM/EDX point microanalysis showed the existence of different crystalline phases inside this thin layer, even along the distance of a few microns. They were mostly of the Cu_2Al_3, CuAl, Cu_3Al_2, Cu_3Al – type.

The more detailed analyses of the chemical composition changes were made on a thicker intermetallic inclusion.

3.4. Chemical composition changes in the intermetallic inclusion

The previous work, based on the SEM observations, shows that the regions of intermetallic inclusion reveal a non-uniform swirl-like contrast of various intensity and thus different chemical compositions [11,16]. To clarify the mechanism of the phase constitution, the energy dispersive X-ray spectrometry in TEM was used for the nano- scale analysis of the distribution of the Cu and Al atoms across the intermetallic layer.

As regards the ‘after bonding’ state, the general observation based on the TEM/EDX measurements is that there was no mechanical mixing between the welded metals in the solid state. The distribution of the elements inside the intermetallic inclusion clearly indicates that some chemical composition fluctuations were observed inside the melted volume. This can be seen in the HAADF/STEM microstructures of Fig. 10. The analysis reveals non-uniform intermixing of the phases, without any interrelation in respect to the parent sheets (Fig. 10a). Strong chemical composition changes were observed even inside the particular dendrites. Figure 10b clearly shows that the core of the dendrites is enriched with Cu and the arms of the dendrite - in Al. The obtained results suggest that, for most of the observed cases, the average copper/aluminium ratio (in at.%) varied from about 3:1 to 1:3, as it was also observed in earlier works, e.g. [15,16]. Two other important conclusions can be drawn. Firstly, the high cooling rates (and the high pressure) lead to the ‘creation’ of crystalline intermetallic phases mostly far from those observed on the

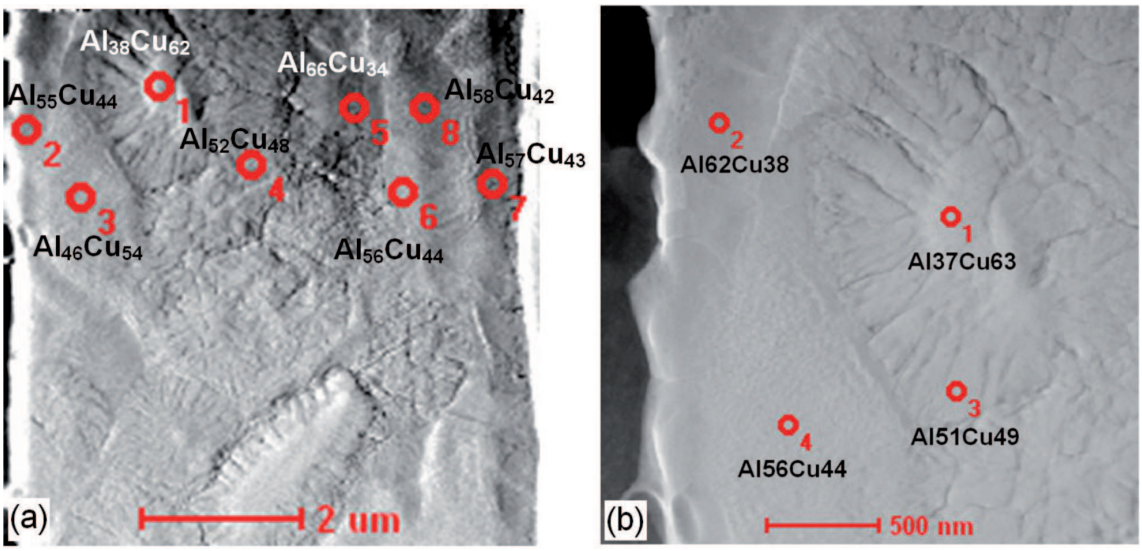

Fig. 10. Chemical composition changes (a) across the whole thickness of the intermetallic inclusion and(b) inside the dendrite near the aluminium sheet (right). HAADF-STEM microstructures and results of the TEM/EDX point microanalysis

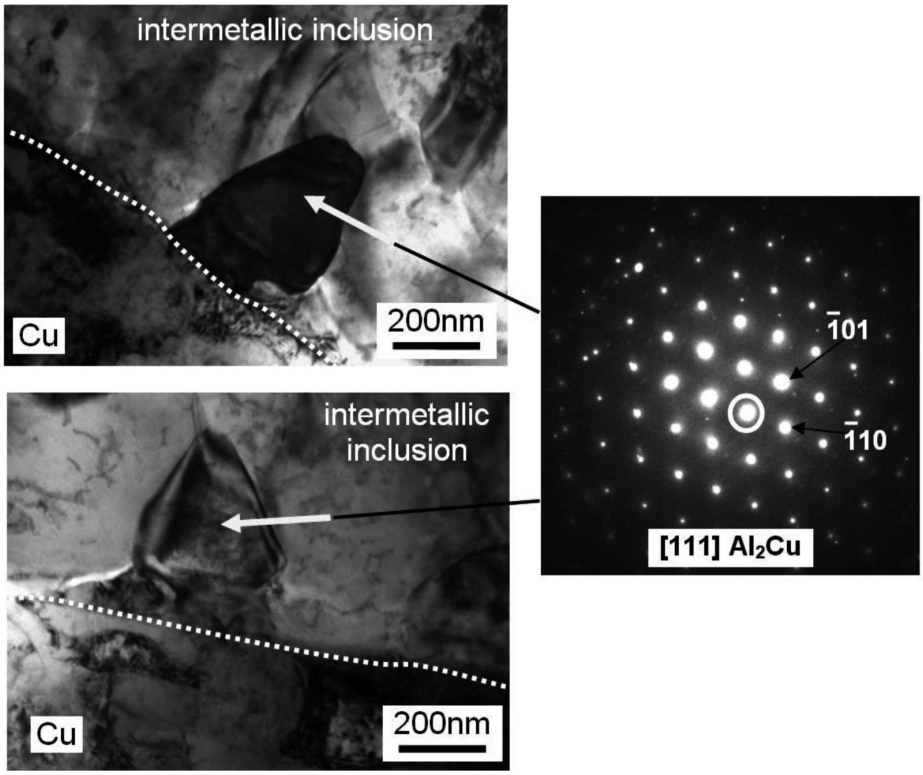

Fig. 11. Micrographs showing microstructure near the Cu/Cu_mAl_n boundary. (a) Nano-grains of the $CuAl_2$ phase growing inwards the intermetallic inclusion. TEM bright field images and the corresponding SAD pattern

equilibrium Cu-Al phase diagram. Secondly, in all the analyzed areas, the intermetallic phases enriched in Al were most often observed. The investigations by means of TEM clearly showed also the presence of three equilibrium intermetallic phases (i.e. the phases that occur in the equilibrium phase diagram), i.e. Θ-$CuAl_2$, γ-Cu_9Al_4 and η-CuAl. Nevertheless, the dominance of the $CuAl_2$ phase is the most important common feature observed in all the analyzed thin foils [17]. The equilibrium phases did not form layers but occupied small, rather irregular, volumes.

This leads to the conclusion that the processes occurring in the liquid state (the intense stir of the melted metals) were prevailing over those observed in the

solid solution. Additionally, the rapid cooling, together with the extremely high pressure, make the solidification terms far from equilibrium and thus influence the occurrence of the 'metastable' phases.

The boundary zone between the solidified melt and the aluminium plate was different from that between the solidified melt and the copper plate. The formation of very small grains (up to 50nm in diameter), growing from the interface to the inside of the intermetallic layer (Fig. 11), was the main feature observed close to the Cu/Cu_mAl_n interface. The chemical composition and the structure of the fine grains mostly fit well to the Al_2Cu phase. The Al/Cu_mAl_n interface was sharper. In that case, the changes in the chemical composition close to the interface, if occurred at all, were too small to be detected by the standard TEM/EDX analysis.

4. Discussion

4.1. Microstructural changes of parent sheets in the layers near the interface

Explosive welding causes a variety of microstructural changes within the bonding zone. One of the most important features is a pronounced increase of the dislocation density and an extremely strong grain refinement in the parent sheets near the interface.

In the present work, two kinds of fine-grained structures were observed. The fine grains of the Al_2Cu phase (probably originating from the liquid state) were observed close to the Cu/Cu_mAl_n interface. However, the grains were growing from the interface to the inside of the intermetallic layer and did not form a compact layer. In the parent sheets, the fine grains were observed in the TEM bright field images in the near-the-interface layers. They were similar to those observed in the SEM/EBSD orientation maps. The orientation maps showed that the grains were separated by large angle grain boundaries with the misorientations higher than 15°. Although the total thickness of this fine-grained zone did not exceed a few microns, the layers showed the well-marked copper-type texture components typically observed in highly deformed fcc metals [12].

The formation of highly dislocated structures and well-defined rolling texture components clearly indicates that the deformation processes dominate over the softening ones and those occurring during the rapid crystallization. The confirmation of this suggestion can be found even in the earlier works based on TEM observations and used for the analysis of the interface morphology in explosively welded sheets. In those works, e.g. [2, 18], the authors observed an increased density of dislocation, a high vacancy concentration and even microtwins, in the parent sheets near the interface [1], i.e. the typical effects accompanying severe plastic deformations.

4.2. Chemical composition changes inside intermetallic inclusion

The general observation resulting from the present research is that the possibility of predicting the formation of the particular phase in the as-bonded state is *unrealistic* or at least '*little realistic*'. This results from the vigorous stirring of the melted volumes due to the high dynamics of the bonding process. But in all the analyzed areas, the intermetallic phases enriched in Al were most often observed. This is probably due to the different solubility of Al in Cu and Cu in Al.

With respect to the changes in the chemical composition, the analysis is strongly dependent on the scale of the observations [10]. The meso- scale analysis based on the energy dispersive X-ray spectrometry in SEM performed in an earlier work [15] indicated that a higher 'average' concentration of copper was observed for the intermetallic inclusions situated in the nearest neighbourhood of the copper plate and a poorer concentration - in the layers situated closer to the aluminium sheet. The above tendency of the chemical composition changes is not so evident for the particular intermetallic inclusion. The micro-/nano- scale analyses performed in this work by means of the TEM/EDX technique documented a strong and unforeseeable differentiation of the chemical composition inside the particular inclusion of the solidified melt. For most of the observed cases, the average copper/aluminium ratio (in at.%) varies from about 3:1 to 1:3, as it was also observed in earlier works, e.g. [11, 16].

4.3. Intermetallic phase formation – comparison with other bonding techniques

Although the metastable phases occupied the major part of the intermetallic inclusion, the equilibrium phases were also observed. However, the diffusion-controlled processes do not play any decisive role in the intermetallic inclusion formation 'in state' just after the deformation bonding. The solid-state transformations can to be crucial for the growth of the intermetallic phases after ageing. The growth kinetics under the conditions close to the equilibrium always leads to a strictly defined sequence of equilibrium intermetallic compounds. The phases enriched with Al were formed close to the Al plate, whereas the phases enriched with Cu – close to the copper plate, e.g. [19]. This regularity of the phase distribution observed under the near equilibrium conditions, is completely 'alien' for explosive welding clads (in the as-bonded state).

The theoretical predictions of the intermetallic phase formation (under the near equilibrium conditions of the solid-state diffusion processes and within a broad range of temperatures) could be based on the free energy values. Since the free energy of formation was negative [19, 21], the Al_4Cu_9 phase was predicted first to be formed at the Cu-Al interface and then on the AlCu and the Al_2Cu phases. However, the experimental observations [19-21] in the diffusion bonded Cu/Al laminates show that Al_2Cu was the first phase which appeared between Cu and Al - before Al_4Cu_9 and AlCu. The differences in the solubility of the elements in the solid solution and the melting temperatures can be the reason why the Al_2Cu phase is more frequently observed in the solidified melt than the other equilibrium phases. Guo et al [19] and Chen et al [21] studied the thermodynamic aspects of the growth of the Al-Cu intermetallic compounds close to the interface after the Cu wire bonding. On the basis of the different solubility of either element, they stated that, since the solubility limit of Cu in Al is an order of magnitude less than that of Al in Cu, the Al(Cu) solid solution would be expected to saturate first, resulting in the preferred nucleation of Al_2Cu. The Al crystals melted as first and solidified later than copper. This causes larger volumes of the Al plate (with respect to Cu) to melt. Therefore, the liquid which was enriched with the Al and Al_2Cu phase was detected more frequently.

5. Conclusions

This work describes the SEM/EBSD and TEM/EDX investigations of the microstructure, the texture and the chemical composition changes near the interface of explosively welded Al and Cu plates. The following detailed conclusions can be drawn.

- During the bond formation, the layers of the parent sheets near the interfaces underwent intense plastic deformation. Consequently, a strong structure refinement was observed in the intermediate layers of both metals. Fine-grained volumes were characterized by the copper-type rolling texture and described by the texture components lying close to the {112}<111>, {123}<634>and {110}<112>orientations. The effect of the grain refinement was clearly observed in copper, whereas aluminium deformed more uniformly in the significant part of the sheet.
- Local melting leads to the formation of intermetallics of different types. The *equilibrium phases* in the form of dendrites of different chemical compositions were always surrounded by *metastable ones* (also crystalline). Moreover, no significant regularity in the phase distribution (inside intermetallic inclusions) with respect to the parent sheets was observed. The latter facts univocally show the dominance of the processes occurring during the intense stirring of the rapidly solidified melt.

Acknowledgements

The authors give thanks to Mr. Z. Szulc and High Energy Technologies Works 'Explomet' (Opole, Poland) for the provision of the Cu/Al clad. The authors are also grateful to Dr J. Wojewoda-Budka (IMIM PAN in Krakow) for the thin foils preparation by FIB.

This work was supported in part by the Polish Ministry of Science and Higher Education (UMO-2012/04/M/ST8/00401).

REFERENCES

[1] T.Z. Blazynski, Explosive Welding, Forming and Compaction, Applied Science Publishers LTD, New York, 1983.
[2] S.H. Carpenter, Shock Waves and High-Strain-Rate Phenomena in Metals, eds. M.A. Meyers, L.E. Murr, Plenum Press, 941-959 New York 1981.
[3] D.G. Brasher, D.J. Butler, A.W. Hare, in Shock Waves for Industrial Applications, ed. L.E. Murr, Noyes Publications, 216-236 (1988).
[4] N.V. Naumovich, A.I. Yadevich, N.M. Chigrinova, in Shock Waves for Industrial Applications, ed. L.E. Murr, Noyes Publications, 170-215 (1988).
[5] A.G. Mamalis, A. Szalay, N.M. Vaxevanidis, D.I. Pantelis, Mat. Sci. Engn. **A188**, 267-275 (1994).
[6] Y. Yang, B. Wang, J. Xiong, J. Mat. Sci. **41**, 3501-3505 (2006).
[7] S.A.A. Akbari Mousavi, S.T.S. Al-Hassani, A.G. Atkins, Materials and Design **29**, 1334-1352 (2008).
[8] S.A.A. Akbari Mousavi, P. Farhadi Sartangi, Materials and Design **30**, 459-468 (2009).
[9] F. Findik, Materials and Design **32**, 1081-1093 (2011).
[10] J. Song, A. Kostka, M. Veehmayer, D. Raabe, Mat. Sci. Engn. **A528**, 2641-2647 (2011).
[11] H. Paul, M. Faryna, M. Prażmowski, R. Bański, Arch. Metall. Mater. **56**, 463-474 (2011).
[12] H. Paul, M. Miszczyk, M. Prażmowski, Z. Szulc, Inżynieria Materiałowa **5**, 1339-1346 (in polish) (2010).
[13] M. Gerland, H.N. Presles, J.P. Guin, D. Bertheau, Mat. Sci. Engn. **A280**, 311-319 (2000).
[14] K. Hokamoto, K. Nakata, A. Mori, R. Tomoshige, S. Tsuda, T. Tsumura, A. Inoue, Journal of Alloys and Compounds **485**, 817-821 (2009).
[15] M. Abbasi, A. Karim Taheri, M.T. Salehi, Journal of Alloys and Compounds **319**, 233-241 (2001).
[16] H. Paul, M. Miszczyk, M. Prażmowski, Mat. Sci. Forum **702-703**, 603-606 (2012).

[17] H. Paul, L. Lityńska-Dobrzyńska, M. Prażmowski, Metall. Mater. Trans A, in print (2013).
[18] L.F. Trueb, J. Appl. Phys. **40**, 2976-2987 (1969).
[19] Y. Guo, G. Liu, H. Jin, Z. Shi, G. Qiao, J. Mater. Sci. **46**, 2467-2473 (2011).
[20] Y. Tanaka, M. Kajihara, Y. Watanabe, Mat. Sci. Engn. **A445-446**, 335-363 (2007).
[21] J. Chen, Y-S. Lai, Y-W. Wang, C.R. Cao, Microelectronics Reliability **51**, 125-129 (2011).

Received: 17 Oktober 2012.